J. Phys. Chem. **1993**, *97*, 5875–5881 **5875**

Ab Initio Study of the Si_2O and Si_3O Molecules

Alexander I. Boldyrev and Jack Simons*

Department of Chemistry, The University of Utah, Salt Lake City, Utah 84112

Received: December 14, 1992

The structures and vibrational frequencies of various structures and electronic states of Si_2O and Si_3O have been studied at the MP2(full)/6-311+G* level, with geometries also calculated at the MP4SDTQ/6-311+G(2df) and QCISD(T)/6-311+G(2df) levels. Triangular Si_2O (C_{2v}, $^1A_1$) and planar-rhombus Si_3O (C_{2v}, $^1A_1$) structures are found to be the most stable, but several other low-lying local minima are also found. The calculated dissociation energies for the lowest energy decompositions of Si_2O into SiO + Si and of Si_3O into Si_2 + SiO are 50.1 and 59.8 kcal/mol, respectively. The energies for $Si_nO \rightarrow Si_n + O$ are much larger. Even the lowest decomposition energies are larger than those found for Li_2O, Li_3O; Mg_2O, Mg_3O; and Al_2O, Al_3O. In both Si_2O and Si_3O, the O atom does not insert into coordination sites of highest symmetry; rather, the most stable structures involve coordination of the O atom to two Si atoms without destroying the Si–Si bonding. Again, this is different than in Li_2O, Li_3O, Mg_2O, Mg_3O, Al_2O, and Al_3O, where the O atom inserts into the site of highest coordination and highest symmetry.

Introduction

Hypermetallic molecules such as Li_nX, Na_nX, K_nX,[1,2] Mg_nX,[3] and Al_nX,[4,5] with electronegative atoms X and with stoichiometries exceeding normal valence expectations have been practiced theoretically and studied experimentally. Metal–metal bonding is found to contribute significantly to the stability of these species. However, similar hyperstoichiometric molecules with nonmetallic ligands are still unknown. One of the important results found in refs 1–3 is that for X = O, the oxygen atom occupies a high-coordination site in which it is bonded to as many other atoms as possible.

In the present work, we investigate the hypersilicon molecules, Si_2O and Si_3O. Experimental and theoretical studies of the SiO monomer and of clusters of Si atoms are extensive,[6–10] and preliminary experimental[11] and theoretical[12] results are available on Si_2O. According to experimental ESR spectra, the Si_2O molecule has a linear SiSiO structure with a triplet $^3\Sigma$ state.[11b] However, in CISD and CASSCF calculations by DeKock and others,[12] the linear symmetric SiOSi triplet ($^3\Sigma^-$) structure is more stable by 10 kcal/mol than the linear asymmetric SiSiO triplet ($^3\Sigma^-$) structure. These authors considered only triplets and found that bent triplet states of SiOSi are higher in energy. We have not been able to find any information on isolated Si_3O. Our interest in these two molecules was stimulated by the fact that they are prototypes of small silicon clusters interacting with an impurity—oxygen atom. Results of our study of such interactions may be of importance to scientists interested in how O atoms and molecules react with various crystal surfaces (or terraces, kinks, or steps) of solid Si.

Computational Details

The geometries of SiO, Si_2, Si_2O, and Si_3O in the singlet and triplet states were first optimized by employing analytical self-consistent-field (SCF) gradients[13] with a polarized split-valence basis set (results at this level are denoted SCF/6-31G*[14,15]) and subsequently at the correlated second-order Møller–Plesset (MP2-(full)) level. Further optimized geometries were obtained using MP2(full) calculations with triple-ζ plus polarization and diffuse bases (denoted 6-311+G*[16,17]).

The fundamental vibrational frequencies, normal coordinates, and zero-point energies (ZPE) were calculated by standard FG matrix methods. Finally, higher quality correlated total energies were evaluated in the frozen-core approximation both by fourth-order Møller–Plesset perturbation theory[18] (MP4) and by the quadratic configuration interaction including singles and doubles with approximate triples QCISD(T)[19] method using 6-311+G-(2df,2p) basis sets. The Gaussian 90 program suite[20] was used to perform all of the calculations, whose results are discussed here.

Results and Discussion

Our calculated molecular properties of the various electronic states of SiO, Si_2, Si_2O, and Si_3O are presented in Tables I–V, and dissociation energies for various decompositions of Si_2, SiO, Si_2O, and Si_3O are shown in Table VI. The corresponding molecular structures are depicted in Figure 1, and the simulated IR spectra of the lowest energy minima of Si_2O and Si_3O are shown in Figure 2.

SiO and Si_2. It is well-known that the SiO molecule has a singlet ($^1\Sigma^+$, $1\sigma^2 2\sigma^2 1\pi^4 3\sigma^2$) ground state and that the Si_2 dimer is a triplet ($^3\Sigma_g^-$, $1\sigma_g{}^2 1\sigma_u{}^2 2\sigma_g{}^2 1\pi_u{}^2$) in its ground electronic state.[6] Our calculated equilibrium bond lengths, vibrational frequencies, and dissociation energies for these two molecules agree with the experimental data to within 0.026 Å (SiO) and 0.009 Å (Si_2), 58 cm^{-1} (SiO) and 4 cm^{-1} (Si_2), and 8 kcal/mol (SiO) and 4 kcal/mol (Si_2), respectively, using MP2(full)/6-311+G* geometries and frequencies and QCISD(T)/6-311+G(2df) total energies. The excitation energy to the first triplet excited state is not known exactly for SiO, but Huber and Herzberg report[6] an estimate of 96.2 kcal/mol. Our best excitation energy of the $^3\Pi$ ($1\sigma^2 2\sigma^2 1\pi^4 3\sigma^1 2\pi^1$) state of this molecule is 97.8 kcal/mol (at the QCISD(T)/6-311+G(2df) level), in good agreement with the recommended value. The first singlet Σ state ($^1\Sigma_g{}^+$, $1\sigma_g{}^2 1\sigma_u{}^2 1\pi_u{}^4$) of Si_2 is known[21] to be higher in energy than the ground state by 16.1 kcal/mol. Again, our best estimate of this excitation energy, 15.8 kcal/mol (QCISD(T)/6-311+G(2df)), is in good agreement.

Si_2O. The valence isoelectronic C_2O molecule is known to have a linear CCO singlet structure.[22] However, for Si_2O we expect another structure to be lower in energy; therefore, triplet and singlet states of linear SiSiO ($C_{\infty v}$) and SiOSi ($D_{\infty h}$) as well as bent SiOSi (C_{2v}) have been studied (see Table II and Figure 1). Because both linear structures have π^2 outer orbital electron configurations, $^1\Delta$ states have been calculated using a small complete active space SCF (from CASSCF(2,2)/6-31G* to CASSCF(6,8)/6-31G*) wave function. This CASSCF wave function does not take into account much correlation energy, but it does give the proper $^1\Delta$ symmetry of the wave function.

0022-3654/93/2097-5875$04.00/0

TABLE I: Calculated Molecular Properties of the Singlet and Triplet States of SiO and Si_2

SiO ($^1\Sigma^+$) $1\sigma^2 2\sigma^2 1\pi^4 3\sigma^2$	SiO ($^3\Pi$) $1\sigma^2 2\sigma^2 1\pi^4 3\sigma^1 2\pi^1$	Si_2 ($^1\Sigma_g^+$) $1\sigma_g^2 1\sigma_u^2 1\pi_u^4$	Si_2 ($^3\Sigma_g^-$) $1\sigma_g^2 1\sigma_u^2 1\pi_u^2 2\sigma_g^2$
MP2(full)/6-311+G*			
R(Si–O() = 1.536 Å	R(Si–O) = 1.506 Å	R(Si–Si) = 2.064 Å	R(Si–Si) = 2.255 Å
$E_{\text{MP2}} = -364.25333$	$E_{\text{MP2}} = -364.09022$	$E_{\text{MP2}} = -578.11043$	$E_{\text{MP2}} = -578.12997$
$\omega_e = 1183$ cm^{-1}	$\omega_e = 2571$ cm^{-1}	$\omega_e = 611$ cm^{-1}	$\omega_e = 506$ cm^{-1}
ZPE = 1.69 kcal/mol	ZPE = 3.68 kcal/mol	ZPE = 0.87 kcal/mol	ZPE = 0.72 kcal/mol
	$\langle S^2 \rangle = 2.029$		$\langle S^2 \rangle = 2.015$
QCISD(T)/6-311+G(2df)			
E_{HF} -363.83286	$E_{\text{PUHF}} = -363.70964$	$E_{\text{HF}} = -577.68053$	$E_{\text{PUHF}} = -577.77116$
$E_{\text{MP2}} = -364.16950$	$E_{\text{PMP2}} = -364.01463$	$E_{\text{MP2}} = -577.90293$	$E_{\text{PMP2}} = -577.92573$
$E_{\text{MP3}} = -364.16001$	$E_{\text{PMP3}} = -364.00623$	$E_{\text{MP3}} = -577.91299$	$E_{\text{PMP3}} = -577.95309$
$E_{\text{MP4}} = -364.19685$	$E_{\text{PMP4}} = -364.03764$	$E_{\text{MP4}} = -577.94145$	$E_{\text{PMP4}} = -577.96470$
$E_{\text{QCISD}} = -364.17365$	$E_{\text{QCISD}} = -364.01895$	$E_{\text{QCISD}} = -577.92081$	$E_{\text{QCISD}} = -577.95618$
$E_{\text{QCISD(T)}} = -364.18964$	$E_{\text{QCISD(T)}} = -364.03377$	$E_{\text{QCISD(T)}} = -577.94191$	$E_{\text{QCISD(T)}} = -577.96713$
D_0(PMP4) = 187.3 kcal/mol	T_e(PMP4) = 99.9 kcal/mol	T_e(PMP4) = 14.6 kcal/mol	D_0(PMP4) = 69.8 kcal/mol
D_0(QCISD(T)) = 182.0 kcal/mol	T_e(QCISD(T)) = 97.8 kcal/mol	T_e(QCISD(T)) = 15.8 kcal/mol	D_0(QCISD(T)) = 69.7 kcal/mol

TABLE II: Calculated Molecular Properties of the Lowest Energy Si_2O Structures

Si_2O (C_{2v}, $^1A_1$) $1a_1^2 2a_1^2 1b_2^2 1b_1^2$- $3a_1^2 2b_2^2 4a_1^2$	Si_2O (C_{2v}, $^3B_1$) $1a_1^2 2a_1^2 1b_2^2 1b_1^2$- $3a_1^2 2b_2^2 4a_1^1 2b_1^1$	SiOSi ($D_{\infty h}$, $^3\Sigma_g^-$) $1\sigma_g^2 1\sigma_u^2 1\pi_u^4$- $2\sigma_g^2 2\sigma_u^2 1\pi_g^2$	Si_2O ($C_{\infty v}$, $^3\Sigma^-$) $1\sigma^2 2\sigma^2 3\sigma^2$- $1\pi^4 3\sigma^2 2\pi^2$
MP2(full)/6-311+G*			
$E_{\text{MP2}} = -653.33286$	$E_{\text{MP2}} = -653.30302$	$E_{\text{MP2}} = -653.30718$	$E_{\text{MP2}} = -653.29342$
$\nu_1(a_1) = 810$ cm^{-1}	$\nu_1(a_1) = 799$ cm^{-1}	$\nu_1(\sigma_g) = 561$ cm^{-1}	$\nu_1(\sigma) = 1207$ cm^{-1}
$\nu_2(a_1) = 437$ cm^{-1}	$\nu_2(a_1) = 353$ cm^{-1}	$\nu_2(\sigma_u) = 967$ cm^{-1}	$\nu_2(\sigma) = 341$ cm^{-1}
$\nu_3(b_2) = 613$ cm^{-1}	$\nu_3(b_2) = 1389$ cm^{-1}	$\nu_3(\pi_u) = 220$ cm^{-1}	$\nu_3(\pi) = 53$ cm^{-1}
ZPE = 2.66 kcal/mol	ZPE = 3.63 kcal/mol	ZPE = 2.81 kcal/mol	ZPE = 2.36 kcal/mol
	$\langle S^2 \rangle = 2.069$	$\langle S^2 \rangle = 2.109$	$\langle S^2 \rangle = 2.035$
QCISD(T)/6-311+G(2df)			
$E_{\text{HF}} = -652.73177$	$E_{\text{PUHF}} = -652.72574$	$E_{\text{PUHF}} = -652.71230$	$E_{\text{PUHF}} = -652.70703$
$E_{\text{MP2}} = -653.15450$	$E_{\text{MP2}} = -653.12835$	$E_{\text{MP2}} = -653.12329$	$E_{\text{MP2}} = -653.11700$
$E_{\text{MP3}} = -653.16393$	$E_{\text{PMP3}} = -653.13846$	$E_{\text{PMP3}} = -653.13413$	$E_{\text{PMP3}} = -653.11951$
$E_{\text{MP4}} = -653.20087$	$E_{\text{PMP4}} = -653.17244$	$E_{\text{PMP4}} = -653.16866$	$E_{\text{PMP4}} = -653.16193$
$E_{\text{QCISD}} = -653.17575$	$E_{\text{QCISD}} = -653.14788$	$E_{\text{QCISD}} = -653.13890$	$E_{\text{QCISD}} = -653.13278$
$E_{\text{QCISD(T)}} = -653.19852$	$E_{\text{QCISD(T)}} = -653.17057$	$E_{\text{QCISD(T)}} = -653.16560$	$E_{\text{QCISD(T)}} = -653.15557$
T_e(PMP4) = 0.0 kcal/mol	T_e(PMP4) = 17.8 kcal/mol	T_e(PMP4) = 20.2 kcal/mol	T_e(PMP4) = 24.4 kcal/mol
T_e(QCISD(T)) = 0.0 kcal/mol	T_e(QCISD(T)) = 17.5 kcal/mol	T_e(QCISD(T)) = 20.7 kcal/mol	T_e(QCISD(T)) = 27.0 kcal/mol

TABLE III: Calculated Molecular Properties of the Lowest Energy Si_3O Structures

Si_3O (D_{3h}, $^1A_1'$) $1a_3'^2 1e'^4 1a_2''^2$- $2a_1'^2 2e'^4 3e'^4$	Si_3O (C_{3v}, $^1A_1$) $1a_1^2 1e^4 2a_1^2 3a_1^2$- $2e^4 3e^4$	Si_3O (C_{2v},I $^1A_1$) $1a_1^2 2a_1^2 1b_2^2$ $1b_1^2 3a_1^2 4a_1^2 2b_2^2$ $5a_1^2 2b_1^2$	Si_3O (C_{2v},II $^1A_1$) $1a_1^2 1b_2^2 2a_1^2$ $1b_1^2 3a_1^2 2b_2^2 4a_1^2$ $3b_2^2 1a_2^2$	Si_3O (C_{2v},I $^3A_2$) $1a_1^2 2a_1^2 1b_2^2 1b_1^2$- $3a_1^2 4a_1^2 2b_2^2 5a_1^2$- $3b_2^1 2b_1^1$	Si_3O (C_{2v}, II $^3B_2$) $1a_1^2 1b_2^2 2a_1^2 1b_1^2$- $3a_1^2 2b_2^2 4a_1^2$- $3b_2^2 2b_1^1 1a_2^1$
MP2(full)/6-311+G*					
$E_{\text{MP2}} = -942.33370$	$E_{\text{MP2}} = -942.36607$	$E_{\text{MP2}} = -942.40014$	$E_{\text{MP2}} = -942.39250^a$	$E_{\text{MP2}} = -942.40049$	$E_{\text{MP2}} = -942.42345^a$
$\nu_1(a_1') = 470$ cm^{-1}	$\nu_1(a_1) = 643$ cm^{-1}	$\nu_1(a_1) = 685$ cm^{-1}	$\nu_1(a_1) = 707$ cm$^{-1\ b}$	$\nu_1(a_1) = 837$ cm^{-1}	$\nu_1(a_1) = 584$ cm$^{-1\ b}$
$\nu_2(a_2'')$ 260i cm^{-1}	$\nu_2(a_1) = 250$ cm^{-1}	$\nu_2(a_1) = 523$ cm^{-1}	$\nu_2(a_1) = 371$ cm$^{-1\ b}$	$\nu_2(a_1) = 514$ cm^{-1}	$\nu_2(a_1) = 458$ cm$^{-1\ b}$
$\nu_3(e') = 755$ cm^{-1}	$\nu_3(e) = 576$ cm^{-1}	$\nu_3(a_1) = 268$ cm^{-1}	$\nu_3(a_1) = 239$ cm$^{-1\ b}$	$\nu_3(a_1) = 355$ cm^{-1}	$\nu_3(a_1) = 286$ cm$^{-1\ b}$
$\nu_4(e')$ 105 cm^{-1}	$\nu_4(e) = 326$ cm^{-1}	$\nu_4(b_1) = 278$ cm^{-1}	$\nu_4(b_1) = 261$ cm$^{-1\ b}$	$\nu_4(b_1) = 156$ cm^{-1}	$\nu_4(b_1) = 174$ cm$^{-1\ b}$
ZPE = 3.13 kcal/mol	ZPE = 3.85 kcal/mol	$\nu_5(b_2) = 194$ cm^{-1}	$\nu_5(b_2) = 2245$ cm$^{-1\ b,c}$	$\nu_5(b_2) = 793$ cm^{-1}	$\nu_5(b_2) = 1961$ cm$^{-1\ b,c}$
		$\nu_6(b_2) = 160i$ cm^{-1}	$\nu_6(b_2) = 295$ cm$^{-1\ b}$	$\nu_6(b_2) = 152$ cm^{-1}	$\nu_6(b_2) = 618$ cm$^{-1\ b}$
		ZPE = 2.78 kcal/mol	ZPE = 5.89 kcal/mol	ZPE = 4.01 kcal/mol	ZPE = 5.83 kcal/mol
MP4SDTQ/6-311+G(2df)					
$E_{\text{SCF}} = -941.51940$	$E_{\text{SCF}} = -941.54331$	$E_{\text{SCF}} = -941.56667$	$E_{\text{SCF}} = -941.52245$	$E_{\text{PUSCF}} = -941.62316$	$E_{\text{PUSCF}} = -941.62216$
$E_{\text{MP2}} = -942.04130$	$E_{\text{MP2}} = -942.09307$	$E_{\text{MP2}} = -942.11095$	$E_{\text{MP2}} = -942.11680$	$E_{\text{PMP2}} = -942.11120$	$E_{\text{MP2}} = -942.14406$
$E_{\text{MP3}} = -942.06559$	$E_{\text{MP3}} = -942.10598$	$E_{\text{MP3}} = -942.12189$	$E_{\text{MP3}} = -942.11279$	$E_{\text{PMP3}} = -942.13262$	$E_{\text{MP3}} = -942.15647$
$E_{\text{MP4}} = -942.10827$	$E_{\text{MP4}} = -942.15806$	$E_{\text{MP4}} = -942.17730$	$E_{\text{MP4}} = -942.18174$	$E_{\text{PMP4}} = -942.17344$	$E_{\text{MP4}} = -942.20502$
$\Delta E_{\text{MP4}} = 94.9$ kcal/mol	$\Delta E_{\text{MP4}} = 63.6$ kcal/mol	$\Delta E_{\text{MP4}} = 51.4$ kcal/mol	$\Delta E_{\text{MP4}} = 48.8$ kcal/mol	$\Delta E_{\text{PMP4}} = 54.0$ kcal/mol	$\Delta E_{\text{PMP4}} = 34.1$ kcal/mol

[a] Frequencies were not calculated at the MP2(full)/6-311+G* level due to difficulties with convergence. [b] Frequencies calculated at the MP2(full)6-31G* level. [c] This frequency is probably overestimated due to multiconfigurational contribution to this mode.

The bent singlet C_{2v} ($^1A_1$, $1a_1^2 2a_1^2 1b_2^2 1b_1^2 3a_1^2 2b_2^2 4a_1^2$) SiOSi structure has been found to be the global minima (see Table II), which is unlike the case for CCO. Five other local minimum structures were also identified, and some of them are characterized in Table II.

The triplet C_{2v} ($^3B_1$, $1a_1^2 2a_1^2 1b_2^2 1b_1^2 3a_1^2 2b_2^2 4a_1^1 2b_1^1$) Si_2O, triplet linear $D_{\infty h}$ ($^3\Sigma_g^-$, $1\sigma_g^2 1\sigma_u^2 1\pi_u^4 2\sigma_g^2 2\sigma_u^2 1\pi_g^2$) SiOSi, and linear $C_{\infty v}$ ($^3\Sigma^-$, $1\sigma^2 2\sigma^2 3\sigma^2 1\pi^4 4\sigma^2 2\pi^2$) SiSiO structures lie higher in energy than the global minimum C_{2v} ($^1A_1$) structure by 17.5, 20.7, and 27.0 kcal/mol, respectively (at the QCISD(T)/6-311+G*(2df) level). The geometrical structure of the C_{2v} ($^3B_1$) triplet state does not differ much from that of the singlet C_{2v} state.

Our results do not agree with the previous conclusion by DeKock and others[12] that the bent triplet SiOSi is higher in energy than the linear molecules. At our largest 6-311+G(2df) basis set, the

TABLE IV: Calculated Molecular Properties of the Lowest Energy Si$_3$O Structures

Si$_3$O ($C_{\infty v}$, $^1\Sigma^+$) $1\sigma^2 2\sigma^2 3\sigma^2 4\sigma^2 1\pi^4$ $5\sigma^2 2\pi^4$	Si$_3$O (C_s, $^1A'$) $1a'^2 2a'^2 3a'^2 4a'^2$ $1a''^2 5a'^2 6a'^2 7a'^2 2a''^2$	Si$_3$O (C_{2v},Y, $^1A_1$) $1a^{12}2a^{12}3a^{12}1b_2^2 1b_1^2$ $2b_2^2 4a_1^2 2b_1^2 5a_1^2$	Si$_3$O (C_{2v}, $\diamond$, $^1A_1$) $1a_1^2 2a_1^2 1b_2^2 3a_1^2$ $1b_1^2 2b_2^2 4a_1^2 5a_1^2 2b_1^2$	Si$_3$O (C_{2v},Y, $^3B_2$) $1a_1^2 2a_1^2 1b_2^2 3a_1^2$ $2b_2^2 4a_1^2 1b_1^2 2b_1^2$ $5a_1^1 3b_2^1$	Si$_3$O (C_{2v}, $\diamond$, $^3B_2$) $1a_1^2 2a_1^2 1b_2^2 3a_1^2$ $1b_1^2 2b_2^2 4a_1^2 2b_1^2$ $5a_1^1 3b_2^1$
			MP2(full)/6-311+G*		
$E_{MP2} = -942.39793$	$E_{MP2} = -942.44698$	$E_{MP2} = -942.44450^a$	$E_{MP2} = -942.47242$	$E_{MP2} = -942.42277$	$E_{MP2} = -942.42809^a$
$\nu_1(\sigma) = 1210\ \mathrm{cm^{-1}}$	$\nu_1(a') = 1204\ \mathrm{cm^{-1}}$	$\nu_1(a_1)\ 1189\ \mathrm{cm^{-1}}\ ^b$	$\nu_1(a_1) = 795\ \mathrm{cm^{-1}}$	$\nu_1(a_1) = 1187\ \mathrm{cm^{-1}}$	$\nu_1(a_1) = 786\ \mathrm{cm^{-1}}\ ^b$
$\nu_2(\sigma) = 631\ \mathrm{cm^{-1}}$	$\nu_2(a') = 525\ \mathrm{cm^{-1}}$	$\nu_2(a_1) = 544\ \mathrm{cm^{-1}}\ ^b$	$\nu_2(a_1) = 527\ \mathrm{cm^{-1}}$	$\nu_2(a_1) = 499\ \mathrm{cm^{-1}}$	$\nu_2(a_1) = 511\ \mathrm{cm^{-1}}\ ^b$
$\nu_3(\sigma) = 315\ \mathrm{cm^{-1}}$	$\nu_3(a') = 454\ \mathrm{cm^{-1}}$	$\nu_3(a_1) = 380\ \mathrm{cm^{-1}}\ ^b$	$\nu_3(a_1) = 461\ \mathrm{cm^{-1}}\ ^b$	$\nu_3(a_1) = 378\ \mathrm{cm^{-1}}$	$\nu_3(a_1) = 366\ \mathrm{cm^{-1}}\ ^b$
$\nu_4(\pi) = 62\ \mathrm{cm^{-1}}$	$\nu_4(a') = 239\ \mathrm{cm^{-1}}$	$\nu_4(b_1) = 172\ \mathrm{cm^{-1}}\ ^b$	$\nu_4(b_1) = 235\ \mathrm{cm^{-1}}$	$\nu_4(b_1) = 199\ \mathrm{cm^{-1}}$	$\nu_4(b_1) = 1794\ \mathrm{cm^{-1}}\ ^b$
$\nu_5(\pi) = 130i\ \mathrm{cm^{-1}}$	$\nu_5(a'') = 144\ \mathrm{cm^{-1}}$	$\nu_5(b_2) = 207\ \mathrm{cm^{-1b}}$	$\nu_5(b_2) = 471\ \mathrm{cm^{-1}}$	$\nu_5(b_2) = 563\ \mathrm{cm^{-1}}$	$\nu_5(b_2) = 759\ \mathrm{cm^{-1}}\ ^b$
ZPE = 3.26 kcal/mol	$\nu_6(a'') = 123\ \mathrm{cm^{-1}}$	$\nu_6(b_2) = 257i\ \mathrm{cm^{-1}}\ ^b$	$\nu_6(b_2) = 306\ \mathrm{cm^{-1}}$	$\nu_6(b_2) = 248\ \mathrm{cm^{-1}}$	$\nu_6(b_4) = 344\ \mathrm{cm^{-1}}\ ^b$
	ZPE = 3.84 kcal/mol	ZPE = 3.56 kcal/mol	ZPE = 3.99 kcal/mol	ZPE = 3.97 kcal/mol	ZPE = 6.52 kcal/mol
			MP4SDTQ/6-311+G(2df)		
$E_{SCF} = -941.55009$	$E_{SCF} = -941.61171$	$E_{SCF} = -941.60632$	$E_{SCF} = -941.64447$	$E_{PUSCF} = -941.61735$	$E_{PUSCF} = -941.64712$
$E_{MP2} = -942.12373$	$E_{MP2} = -942.17300$	$E_{MP2} = -942.17002$	$E_{MP2} = -942.19960$	$E_{PMP2} = -942.15097$	$E_{PMP2} = -942.16077$
$E_{MP3} = -942.11520$	$E_{MP3} = -942.17363$	$E_{MP3} = -942.17025$	$E_{MP3} = -942.20671$	$E_{PMP3} = -942.15519$	$E_{PMP3} = -942.17457$
$E_{MP4} = -942.18928$	$E_{MP4} = -942.23197$	$E_{MP4} = -942.22954$	$E_{MP4} = -942.25944$	$E_{PMP4} = -942.20767$	$E_{PMP4} = -942.21895$
ΔE_{MP4} = 44.0 kcal/mol	ΔE_{MP4} = 17.2 kcal/mol	ΔE_{MP4} = 18.8 kcal/mol	ΔE_{MP4} = 0.0 kcal/mol	ΔE_{MP4} = 32.5 kcal/mol	ΔE_{MP4} = 25.4 kcal/mol

[a] Frequencies were not calculated at the MP2(full)/6-311+G* level due to problems with convergence. [b] Frequencies calculated at the MP2(full)/6-31G* level.

TABLE V: Calculated Molecular Properties of the Lowest Energy Si$_3$O Structures

Si$_3$O (C_{3v}, $^3A_1$) $1a_1^2 2a_1^2 1e^4 3a_1^2 2e^4 4a_1^2 3e^2$	Si$_3$O (C_{2v},III $^1A_1$) $1a_1^2 1b_2^2 2a_1^2 1b_1^2$- $3a_1^2 2b_2^2 4a_1^2 3b_2^2 2b_1^2$
MP2(full)/6-311+G*	
$E_{MP2} = -942.41130^a$	$E_{MP2} = -942.42368$
$\nu_1(a_1) = 756\ \mathrm{cm^{-1}}\ ^b$	$\nu_1(a_1) = 589\ \mathrm{cm^{-1}}$
$\nu_2(a_1) = 432\ \mathrm{cm^{-1}}\ ^b$	$\nu_2(a_1) = 409\ \mathrm{cm^{-1}}$
$\nu_3(e) = 401\ \mathrm{cm^{-1}}\ ^b$	$\nu_3(a_1) = 314\ \mathrm{cm^{-1}}$
$\nu_4(e) = 236\ \mathrm{cm^{-1}}\ ^b$	$\nu_4(b_1) = 33\ \mathrm{cm^{-1}}$
ZPE = 3.52 kcal/mol	$\nu_5(b_2) = 591\ \mathrm{cm^{-1}}$
$\langle S^2 \rangle = 2.048$	$\nu_6(b_2) = 262i\ \mathrm{cm^{-1}}$
	ZPE = 2.62 kcal/mol
MP4SDTQ/6-311+G(2df)	
$E_{PUSCF} = -941.61980$	$E_{SCF} = -941.60273$
$E_{PMP2} = -942.14451$	$E_{MP2} = -942.14494$
$E_{PMP3} = -942.15613$	$E_{MP3} = -942.15653$
$E_{PMP4} = -942.20460$	$E_{MP4} = -942.20898$
ΔE_{PMP4} = 34.4 kcal/mol	ΔE_{PMP4} = 31.7 kcal/mol

[a] Frequencies were not calculated at the MP2(full)/6-311+G* level due to problems with convergence. [b] Frequencies calculated at the MP2(full)/6-31G*.

bent C_{2v} ($^3B_1$) structure of Si$_2$O is more stable than the linear $D_{\infty h}$ ($^3\Sigma_g^-$) at all levels of theory, from PUSCF to QCISD(T). In our calculation, we also found that the linear SiOSi ($D_{\infty h}$, $^3\Sigma_g^-$) structure is more stable than SiSiO ($C_{\infty v}$, $^3\Sigma^-$), as in the previous calculations by DeKock and others.[12] However, we emphasize that neither the C_{2v} ($^3B_1$) structure nor the $D_{\infty h}$ ($^3\Sigma_g^-$) structure of Si$_2$O is the global minimum.

The CASSCF(6,8)/6-31G* (1176 CSFs (configuration state functions) for the singlet state and 1512 CSFs for the triplet state) calculations at the SCF/6-31G* geometry have shown that the Hartree–Fock function dominates in the singlet C_{2v}, $^1A_1$ state ($C_{HF} = 0.948$) and in the triplet C_{2v}, $^3B_1$ ($C_{HF} = 0.950$) state. Therefore, our results based on the MP4 and QCISD(T) methods should be reliable. At the CASSCF(6,8)/6-31G* level, the singlet C_{2v} ($^1A_1$) structure is more stable than the triplet C_{2v} ($^3B_1$) one by 23.4 kcal/mol.

The $^1\Delta$ states of SiOSi ($^1\Delta_g$, $1\sigma_g^2 1\sigma_u^2 1\pi_u^4 2\sigma_g^2 2\sigma_u^2 1\pi_g^2$) at the CASSCF(2,4)/6-31G*, CASSCF(6,6)/6-31G*, and CASSCF-(6,8)/6-31G* levels (in the former case the singlet state has 1176 CSFs and the triplet state has 1512 CSFs) lie 3.0, 2.9, and 3.6 kcal/mol, respectively, above the $^3\Sigma_g^-$ state of SiOSi (at the CASSCF(2,2)/6-31G* geometry). However, both states are not well represented by the Hartree–Fock wave function: C_{HF} = 0.866 in the CASSCF(6,8)/6-31G* expansion for the $^3\Sigma_g^-$ state, while two configurations with $1\pi_{ux}^2$ and $1\pi_{uy}^2$ occupations (coefficients are 0.587) dominate in the $^1\Delta_g^-$ state.

The $^1\Delta$ state of SiSiO ($^1\Delta^-$, $1\sigma^2 2\sigma^2 3\sigma^2 1\pi^4 4\sigma^2 2\pi^2$) at the CASSCF(2,6)/6-31G*, CASSCF(4,6)/6-31G*, and CASSCF-(4,8)/6-31G* levels lies 16.0, 16.7, and 16.5 kcal/mol, respectively, above the $^3\Sigma^-$ state of SiSiO (again at CASSCF(2,2)/6-31G* geometry). The triplet state is well represented by Hartree–Fock function (C_{HF} = 0.976 in CASSCF(4,8)/6-31G* expansion), but the singlet requires a two-determinant wave function with $1\pi_x^2$ and $1\pi_y^2$ occupations. Therefore, in our high-level calculations, only triplet states of linear SiOSi and SiSiO have been studied.

The bent singlet-state global minimum of the Si$_2$O molecule is thermodynamically stable with respect to dissociation into SiO-($^1\Sigma^+$) + Si(^{3}P) by 50.1 kcal/mol (this value is somewhat less than D_e(Si$_2$) = 74.7 kcal/mol), as well as into Si$_2$($^3\Sigma_g^-$) + O(^{3}P) by 162.4 kcal/mol.

The equilibrium Si–Si bond length (2.340 Å) in Si$_2$O (C_{2v}, $^1A_1$) is close to the "normal" Si–Si single bond in H$_3$Si–SiH$_3$ (2.337 Å), and the Si–O distances (1.723 Å) are also close to the normal single Si–O bonds in H$_3$Si–OH (1.661 Å all at MP2-(full)/6-311++G** level). Therefore, the bonding in this molecule may be represented as a single Si–Si bond and two single Si–O bonds with one lone electron pair on each silicon atom. The calculated infrared (IR) spectrum is presented in Figure 2 to help identify this molecule in the gas phase or in matrix isolation.

The lowest energy Si$_2$O structure is different from those of Li$_2$O, Mg$_2$O, and Al$_2$O, in which the oxygen atom breaks the metal–metal bond to form stable linear X–O–X structures. In Si$_2$O, the oxygen is coordinated to both Si atoms, but a single Si–Si bond remains intact. This result provides us the first hint that when oxygen atoms interact with larger silicon clusters, they will coordinate outside of rather than insert into such clusters.

Si$_3$O. Isolated Si$_3$ clusters have previously been studied by ab initio methods,[10b] and the ground state was found to be cyclic (C_{2v}, $^1A_1$) with an apex bond angle of 77.2° and an Si–Si bond length of 2.179 Å. The linear structure of Si$_3$ is found to be a saddle point which rearranges without activation to the $^1A_1$ cyclic structure. There is a low-lying triangular triplet state (D_{3h}, $^3A_2'$) which lies only a few kcal/mol above the $^1A_1$ ground state.

Our calculated geometrical parameters for Si$_3$ (C_{2v}, $^1A_1$) give an apex bond angle of 78.4°, an Si–Si bond length of 2.173 Å, and calculated vibrational frequencies of $\nu_1(a_1) = 579\ \mathrm{cm^{-1}}$, $\nu_2(a_1) = 195\ \mathrm{cm^{-1}}$, and $\nu_3(b_2) = 562\ \mathrm{cm^{-1}}$ (all at the MP2(full)/6-311+G* level).

TABLE VI: Calculated (with 6-311+G(2df) Basis Set) and Experimental Dissociation Energies of the Si_nO Species (kcal/mol)

reaction	PUHF	PMP2	PMP3	PMP4	QCISD(T)	QCISD(T)+ZPE	expt[a]
$Si_2 \rightarrow Si + Si$	39.8	68.9	68.9	70.4	70.5	69.7	74.0
$SiO \rightarrow Si + O$	104.7	194.3	171.1	189.0	183.7	182.0	190.0
$Si_2O \rightarrow SiO + Si$	28.3	48.3	51.7	48.8	51.1	50.1	
$Si_2O \rightarrow Si_2 + O$	93.1	173.8	153.8	167.3	164.3	162.4	
$Si_2O \rightarrow 2Si + O$	133.0	242.6	222.7	237.8	234.8	232.2	
$Si_3O \rightarrow Si_2O + Si$	36.9	86.0	76.0	83.0		81.7[b]	
$Si_3O \rightarrow SiO + Si_2$	25.4	65.5	58.7	61.4		59.8[b]	
$Si_3O \rightarrow Si_3$[c] $+ O$	94.0	161.6	143.1	155.3		153.2[b]	
$Si_3O \rightarrow 3Si + O$	169.9	328.7	298.8	320.8		316.8[b]	

[a] Experimental data from ref 6. [b] At the MP4SDTQ/6-311+(2df)//MP2(full)/6-311+G*+ZPE level. [c] Geometries and frequencies of Si_3 calculated at the MP2(full)/6-311+G* level.

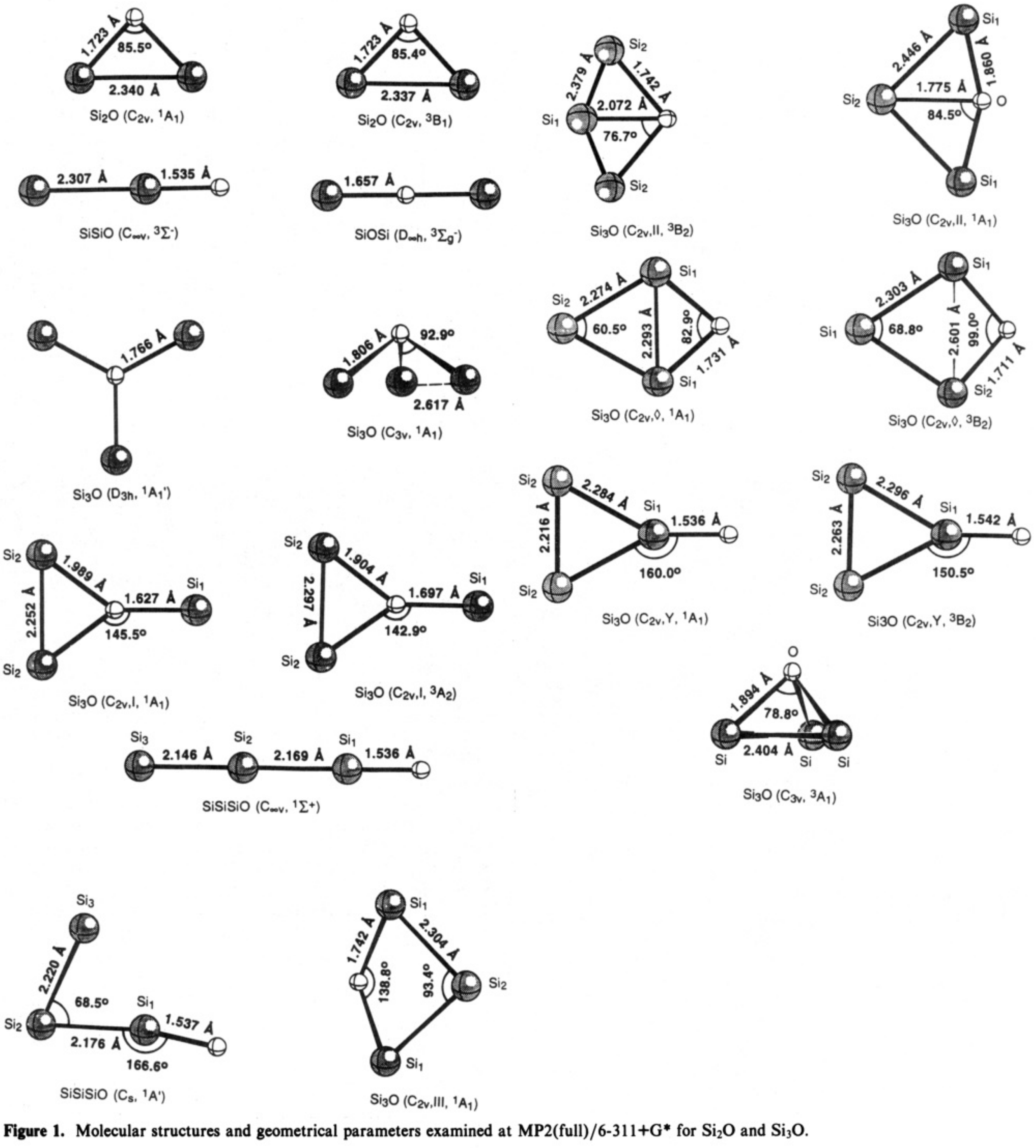

Si_2O (C_{2v}, $^1A_1$)

Si_2O (C_{2v}, $^3B_1$)

Si_3O (C_{2v},II, $^3B_2$)

Si_3O (C_{2v},II, $^1A_1$)

SiSiO ($C_{\infty v}$, $^3\Sigma^-$)

SiOSi ($D_{\infty h}$, $^3\Sigma_g^-$)

Si_3O (D_{3h}, $^1A_1'$)

Si_3O (C_{3v}, $^1A_1$)

Si_3O (C_{2v},◊, $^1A_1$)

Si_3O (C_{2v},◊, $^3B_2$)

Si_3O (C_{2v},Y, $^1A_1$)

Si3O (C_{2v},Y, $^3B_2$)

Si_3O (C_{2v},I, $^1A_1$)

Si_3O (C_{2v},I, $^3A_2$)

Si_3O (C_{3v}, $^3A_1$)

SiSiSiO ($C_{\infty v}$, $^1\Sigma^+$)

SiSiSiO (C_s, $^1A'$)

Si_3O (C_{2v},III, $^1A_1$)

Figure 1. Molecular structures and geometrical parameters examined at MP2(full)/6-311+G* for Si_2O and Si_3O.

Threefold Coordinated Oxygen. The first structures examined for Si_3O (see Figure 1) involve the insertion of an oxygen atom into the triangle of Si_3 in a threefold site. The resultant high-symmetry D_{3h} structure ($^1A_1$, $1a_1'^2 1e'^4 1a_2''^2 2a_1'^2 2e'^4 3e'^4 2a_2''^0$)

was found to have one imaginary vibrational frequency $\nu_2(a_2'')$; allowing this mode to distort leads to a pyramidal C_{3v} ($^1A_1$, $1a_1^2 1e^4 2a_1^2 3a_1^2 2e^4 3e^4 4a_1^0$) local minimum which is 31.3 kcal/mol lower in energy. However, the Si–Si distances (2.617 Å) in the C_{3v} ($^1A_1$) structure are larger than single Si–Si bonds in molecules such as H_3Si–SiH_3 (R(Si–Si) = 2.337 Å). Therefore, silicon–silicon interactions do not contribute significantly to the stability of this structure. Probably as a result, this C_{3v} ($^1A_1$) structure is not thermodynamically stable with respect to dissociation into SiO + Si_2 (i.e., its lowest energy decomposition path).

Deforming the D_{3h} singlet structure while retaining planar symmetry leads to two lower energy structures: C_{2v},I ($^1A_1$, $1a_1^2 2a_1^2 1b_2^2 1b_1^2 3a_1^2 4a_1^2 2b_2^2 5a_1^2 2b_1^2$) and C_{2v},II ($^1A_1$, $1a_1^2 1b_2^2 2a_1^2 1b_1^2 3a_1^2 2b_2^2 4a_1^2 3b_2^2 1a_2^2 1b_1^0$). In the C_{2v},I ($^1A_1$) structure, two Si–Si bonds elongate (by 0.429 Å) and one Si–Si bond shortens (by 0.773 Å) relative to the D_{3h} starting point. As a result, two silicon atoms approach close enough (R(Si–Si) = 2.253 Å) to form a bond. In the C_{2v},II ($^1A_1$) structure, one silicon–silicon distance increases, relative to the D_{3h} starting point, but the two other decrease to form two Si–Si single bonds (R(Si–Si) = 2.446 Å). The C_{2v},I ($^1A_1$) structure is a saddle point, and the C_{2v},II ($^1A_1$) structure is a local minimum (see Tables III–V).

In contrast, the triplet states C_{2v},I ($^3A_2$, $1a_1^2 2a_1^2 1b_2^2 3a_1^2 4a_1^2 2b_2^2 5a_1^2 3b_2^1 2b_1^1 1a_2^0$) and C_{2v},II ($^3B_2$, $1a_1^2 1b_2^2 2a_1^2 1b_1^2 3a_1^2 2b_2^2 4a_1^2 3b_2^2 1a_2^2$) corresponding to these two C_{2v} structures are both local minima. However, the most stable of these structures, C_{2v},II ($^3B_2$), lies only 27.3 kcal/mol below the energy of the dissociation products SiO + Si_2. From these data, we speculated that lower energies might arise from structures that do not place the oxygen atom inside the silicon cluster; again, this is unlike Na_3O, Mg_3O, and Al_3O, where the most stable structures have the oxygen atom inside the cluster.

Another C_{3v} pyramidal structure involves binding of the oxygen atom in a threefold site of Si_3 without breaking the silicon–silicon bonds (see Tables III–V). The corresponding C_{3v} ($^3A_1$, $1a_1^2 2a_1^2 1e^4 3a_1^2 2e^4 4a_1^2 3e^2$) structure is a local minimum but lies ~34.4 kcal/mol (at the (MP4SDTQ/6-311+G(2df) level) higher in energy than the global minimum C_{2v},◊ ($^1A_1$) structure, to be discussed shortly.

Twofold Coordinated Oxygen. Structures in the next group examined begin by coordinating the oxygen atom to the exterior (edges and vertices) of the most stable C_{2v} ($^1A_1$) structure of Si_3. Both singlet and triplet structures have been optimized, and our findings are summarized in Tables III–V.

A singlet rhombus C_{2v},◊ ($^1A_1$, $1a_1^2 2a_1^2 1b_2^2 3a_1^2 1b_1^2 2b_2^2 4a_1^2 5a_1^2 2b_1^2$) structure (Figure 1) with the oxygen atom coordinated to an edge of the Si_3 triangle was found to be the most stable structure. The optimized Si_1–O (1.731 Å) and Si_1–Si_1 bonds (2.311 Å) as well as the angle ∠Si_1OSi_1 (82.9°) are very close to the corresponding Si–O (1.723 Å) and Si–Si (2.340 Å) bond lengths and angles ∠SiOSi (85.5°) in the most stable structure of Si_2O (see Tables II and III–V). All silicon–silicon bond lengths are comparable to "normal" single Si–Si bond lengths.

Singly Coordinated Oxygen. In the vertex-bonded structure C_{2v},Y ($^1A_1$, $1a_1^2 2a_1^2 3a_1^2 1b_2^2 1b_1^2 2b_2^2 4a_1^2 2b_1^2 5a_1^2$) shown in Figure 1, the oxygen atom is coordinated to only one of the Si atoms. The oxygen–silicon bond (1.536 Å) is 0.20 Å shorter than that in the C_{2v},◊ ($^1A_1$) rhombus structure and is the same as that in diatomic SiO (1.536 Å at the MP2(full)/6-311+G* level). The Si_1–Si_2 bond length (2.284 Å) is close to the length of normal single Si–Si bonds, and the Si_2–Si_2 bond length is 0.07 Å shorter. However, this C_{2v},Y ($^1A_1$) structure is a saddle point whose Hessian eigenvector of imaginary frequency leads to the twofold coordinated C_{2v},◊ ($^1A_1$) structure discussed earlier. The barrier for the intramolecular movement of the oxygen atom between the C_{2v},◊ and Y structures is high (18.8 kcal/mol at QCISD(T)/6-311+G(2df) level) and probably too high to display rovibrational spectral manifestations.

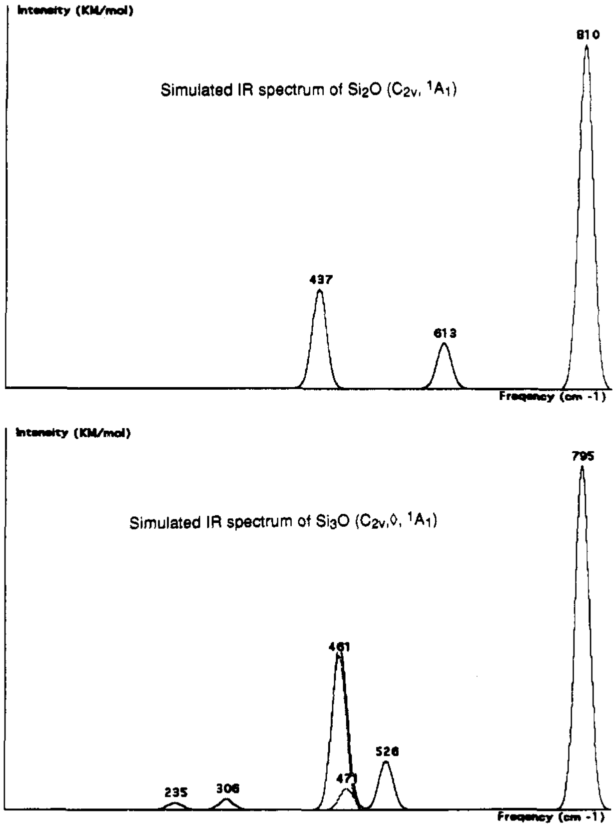

Figure 2. Calculated infrared absorption spectrum for the lowest energy structures of Si_2O and Si_3O.

The triplet C_{2v},◊ ($^3B_2$, $1a_1^2 2a_1^2 1b_2^2 3a_1^2 1b_1^2 2b_2^2 4a_1^2 2b_1^2 5a_1^1 3b_2^1$) and C_{2v},Y ($^3B_2$, $1a_1^2 2a_1^2 1b_2^2 3a_1^2 2b_2^2 4a_1^2 1b_1^2 5a_1^2 2b_1^2 3b_2^2$) structures are higher in energy by 25.4 and 13.7 kcal/mol (at MP4SDTQ/6-311+G(2df)) than the corresponding singlet structures. The triplet C_{2v},◊ ($^3B_2$) and C_{2v},Y ($^3B_2$) structures are local minima.

Linear Structures. Next, we examined linear SiSiSiO structures, since the carbon analog CCCO is known to have a linear structure from both experimental[24] data (involving λ-doubling of vibrationally excited bending states) and ab initio results[23] (at the MP3/6-31G* level), although strong bending anharmonicity has also been noted.[24]

The singlet linear SiSiSiO structure ($^1\Sigma^+$, $1\sigma^2 2\sigma^2 3\sigma^2 4\sigma^2 1\pi^4 5\sigma^2 2\pi^4 3\pi^0$) was found to have two imaginary frequencies $\nu_5(\pi)$ which lead, via a planar trans deformation, to a C_s ($^1A'$, $1a'^2 2a'^2 3a'^2 4a'^2 1a''^2 5a'^2 6a'^2 7a'^2 2a''^2 8a'^0$) minimum-energy structure (see Figure 1). This C_s ($^1A'$) structure is a local minimum which is only 17.2 kcal/mol above the rhombus global minimum detailed earlier. The barrier connecting this structure and the linear structure is high (26.8 kcal/mol).

Thermodynamic Stability of the Lowest Energy Si_3O Structure. The lowest energy C_{2v},◊ ($^1A_1$) structure identified above is stable with respect to all dissociation paths. Its calculated dissociation energy is 81.7 kcal/mol into Si_2O + Si, 59.8 kcal/mol into SiO + Si_2, and 153.2 kcal/mol into Si_3 + O at the MP4SDTQ/6-311+G(2df)+ZPE level. Therefore, this structure of Si_3O is a viable species that should be amenable to gas-phase or inert matrix experiments. The simulated IR spectrum shown in Figure 2 may help in such identification.

For the lowest C_{2v} ($^1A_1$) structure, we carried out CASSCF-(6,8)/6-31G* calculations at the SCF/6-31G* geometry. The Hartree–Fock function was found to dominate (C_{HF} = 0.932) in the CASSCF expansion, so our results at the MP4 and QCISD-(T) levels should be reliable.

Recently, the Si_3C molecule has been studied experimentally[25] and theoretically.[26] Its calculated lowest energy structure and vibrational spectrum agree well with the experimental data. A rhombus C_{2v} ($^1A_1$) minimum-energy structure has been found for Si_3C; this structure can be viewed as the rhombus D_{2h} (^1A_g) structure of Si_4 in which one carbon atom is replaced by a silicon atom. The Si_3O molecule examined here has a similar rhombus structure; however, the chemical bonding is different in Si_3O and Si_3C. In Si_3C, the carbon atom is coordinated to all three silicon atoms and silicon–silicon bonding between the two bridge atoms is absent; in Si_3O, the oxygen atom is coordinated to only two silicon atoms and silicon–silicon bonding between the two bridge atoms is retained (as evidenced by the Si–Si bond lengths).

Overview

Si_2O and Si_3O may provide prototypes for the interation between an O atom and the simplest silicon clusters or sites that are accessible on various solid silicon surfaces, kinks, steps, and terraces. Therefore, it is important to now compare results of our calculations with available experimental data on oxygen chemisorption to silicon surfaces. We begin by summarizing our results.

Our Findings. First, we found that the most energetically stable structures involve an oxygen atom coordinated to two silicon atoms on the periphery of the cluster. This twofold coordination is favored over monodentate coordination, which, in turn, is favored over threefold coordination.

We found that the energy required to desorb atomic oxygen or atomic silicon is much higher than the energy required for desorbtion of an intact SiO molecule. Thus, SiO should be the most abundant species observed in desorption from oxidized silicon surface.

We calculated vibrational frequencies of the Si–O–Si symmetric stretch (810 cm^{-1}) and antisymmetric stretch (613 cm^{-1}) vibrations for the lowest energy bent structure of Si_2O; our calculations produced 705 and 471 cm^{-1}, respectively, for these vibrations in the lowest energy rhombus structure of Si_3O. In contrast, the calculated Si–O frequency of the monodentate–bonded structure of Si_2O is 1207 cm^{-1}; for monodentate-bonded Si_3O, it is 1189 cm^{-1}.

Experimental Information. In a real-time study of oxygen reacting with Si(100) by Yu and Eldridge,[27] only SiO was detected as a desorbed reaction product. This result has been supported by other experimental observations.[28] The energy required to activate the SiO desorption process from Si(100) was found to be 69 kcal/mol,[27] which is similar to our $Si_3O \rightarrow Si_2 + SiO$ dissociation energy (60 kcal/mol).

On silicon surfaces, two types of oxides have been observed by high-resolution electron energy loss spectroscopy, ultraviolet photoelectron spectroscopy, and low-energy electron diffraction.[29] A feature corresponding to an energy loss of 1226 cm^{-1} was attributed to one oxide, and features at 444, 686, and 1032 cm^{-1} were attributed to a second oxide.[29a]

The former oxide is consistent with diatomic SiO adsorbed on the surface. Its 1226-cm^{-1} band is close to the vibrational frequencies we obtain for monodentate-bonded species (e.g., 1183 cm^{-1} in SiO, 1207 cm^{-1} in Si_2O ($C_{\infty v}$, $^3\Sigma^-$), 1190 cm^{-1} in Si_3O (C_{2v}, Y, $^1A_1$), and 1187 cm^{-1} in Si_3O (C_{2v}, Y, $^3B_2$)).

The second oxide was proposed to closely resemble SiO in a local environment similar to that in bulk silicon monoxide. While the nature of the bulk SiO is still controversial, Yasaitis and Kaplow[30] and Bianconi and Bauer[31] concluded that their X-ray diffraction data are consistent with ring structures involving $(SiO)_n$ in which each oxygen atom is coordinated to two silicon atoms and in which there is substantially reduced Si–Si bonding. Our calculated frequencies for the twofold coordinated lowest energy structures of Si_2O ($\nu_1(a_1)$ = 810 cm^{-1} (symmetric stretch O–Si_2 vibration), $\nu_3(b_2)$ = 613 cm^{-1} (asymmetric stretch O–Si_2 vibration), and $\nu_2(a_1)$ = 437 cm^{-1} (symmetric stretch Si–Si vibration)) and Si_3O ($C_{2v},\diamond$, $^1A_1$) ($\nu_1(a_1)$ = 795 cm^{-1} (symmetric stretch O–Si_2 vibration), $\nu_5(b_2)$ = 471 cm^{-1} (asymmetric stretch O–Si_2 vibration), and $\nu_3(a_1)$ = 461 cm^{-1} (symmetric stretch Si–Si vibration)) are similar to the observed vibrational bands ascribed to the second oxide (1065, 686, and 428 cm^{-1} in ref 29a and 992, 871, 774, and 403 cm^{-1} in ref 29b). In particular, the Si–Si vibrational frequencies seem to match well. Therefore, it seems most likely that, in this oxide, each O atom resides in a twofold coordination site in which significant Si–Si bonding is intact.

Conclusions

The results of our calculations on Si_2O and Si_3O have shown that an oxygen atom favors coordination to the periphery of silicon clusters rather than insertion into Si–Si bonds. Structures with the oxygen atom inside the cluster that result in rupture of Si–Si bonding are much higher in energy. This result is in sharp contrast with the structures of other oxygen–metal clusters, such as Li_3O, Li_4O, Mg_2O, Mg_3O, Mg_4O, Al_2O, Al_3O, and Al_4O, where the most stable structures have the oxygen atom in the interior of the cluster in a high-coordination location.

Particularly important findings include the following:

(1) Si_2O and Si_3O are thermodynamically stable species with singlet triangular C_{2v} ($^1A_1$) and planar-rhombus $C_{2v},\diamond$ ($^1A_1$) structures, respectively. Therefore, they are viable molecules that might be found in gas-phase and matrix isolation experiments.

(2) The lowest energy decomposition path for both species involves loss of an SiO molecule. For $Si_3O \rightarrow SiO + Si_2$, the energy difference is 60 kcal/mol, and for $Si_2O \rightarrow SiO + Si$ it is 50 kcal/mol. For Si_3O, loss of atomic Si or of O requires 82 or 153 kcal/mol, respectively.

(3) All structures of Si_3O with the oxygen atom inside the Si_3 cluster are less stable than the planar-rhombus $C_{2v},\diamond$ ($^1A_1$) structure in which the oxygen atom is coordinated to an edge of Si_3 cluster.

(4) Structures with the O atom coordinated to a single Si site are less stable than the twofold coordinated species but more stable than the threefold coordinated species.

(5) Our computed vibrational frequencies seem to shed light on the geometrical and bonding nature of two oxide structures that have been studied experimentally.

It is our hope that the results presented here stimulate further experimental study of small Si_nO clusters, where results of such calculations may be useful guides to interpreting the experimental data.

Acknowledgment. This work was supported in part by the Office of Naval Research and National Science Foundation Grant CHE9116286. The authors thank D. A. Boldyrev for coding the program for simulating IR spectra.

References and Notes

(1) (a) Schleyer, P. v. R.; Wurthwein, E.-U.; Pople, J. A. *J. Am. Chem. Soc.* **1982**, *104*, 5839. (b) Schleyer, P. v. R. In *New Horizons of Quantum Chemistry*; Lowdin, P.-O., Pullman, A., Eds.; Reidel: Dordrecht, The Netherlands, 1983; pp 95–105. (c) Schleyer, P. v. R.; Wurthwein, E.-U.; Kaufmann, E.; Clark, T. *J. Am. Chem. Soc.* **1983**, *105*, 5930. (d) Gutsev, G. L.; Boldyrev, A. I. *Chem. Phys. Lett.* **1982**, *92*, 262. (e) Wurthwein, E.-U.; Schleyer, P. v. R. *J. Am. Chem. Soc.* **1984**, *106*, 6973. (f) Pewestorf, W.; Bonacic-Koutecky, V.; Koutecky, J. *J. Chem. Phys.* **1988**, *89*, 5794. (g) Fantucci, P.; Bonacic-Koutecky, V.; Pewerstort, W.; Koutecky, J. *J. Chem. Phys.* **1989**, *91*, 4229. (h) Klimenko, N. M.; Musaev, D. G.; Gorbik, A. A.; Zyubin, A. S.; Charkin, O. P.; Wurthwein, E.-U.; Schleyer, P. v. R. *Koord. Khim.* **1986**, *12*, 601. (i) Savin, A.; Preuss, H.; Stoll, H. *Rev. Roum. Chim.* **1987**, *32*, 1069. (j) Zakrzewski, V. G.; Niessen, W. v.; Boldyrev, A. I.; Schleyer, P. v. R. *Chem. Phys. Lett.* **1992**, *197*, 195. (k) Rehm, E.; Boldyrev, A. I.; Schleyer, P. v. R. *Inorg. Chem.* **1992**, *31*, 4834.

(2) (a) Wu, C. H.; Kudo, H.; Ihle, H. R. *J. Chem. Phys.* **1979**, *70*, 1815. (b) Wu, C. H. *Chem. Phys. Lett.* **1987**, *139*, 357. (c) Peterson, K. I.; Dao, P. D.; Castleman, A. W., Jr. *J. Chem. Phys.* **1983**, *79*, 777. (d) Dao, P. D.; Peterson, K. I.; Castleman, A. W., Jr. *J. Chem. Phys.* **1984**, *80*, 563. (e) Kudo, H.; Wu, C. H. *Chemistry Express* **1990**, *5*, 633. (f) Kudo, H.; Zmbov, K. F. *Chem. Phys. Lett.* **1991**, *187*, 77. (g) Kudo, H. *Nature* **1992**, *355*, 432.

(3) Boldyrev, A. I.; Shamovsky, I. L.; Schleyer, P. v. R. *J. Am. Chem. Soc.* **1992**, *114*, 6469.

(4) Boldyrev, A. I.; Schleyer, P. v. R. *J. Am. Chem. Soc.* **1991**, *113*, 9045.

(5) Cox, D. M.; Trevor, D. J.; Whetten, R. L.; Rohlfing, E. A.; Kaldor, A. *J. Chem. Phys.* **1986**, *84*, 4651.

(6) Huber, K. P.; Herzberg, G. *Molecular Spectra and Molecular Structure. IV. Constants of Diatomic Molecules*; Van Nostrand Reinhold: New York, 1979.

(7) (a) Anderson, J. S.; Ogden, J. S.; Ricks, M. J. *Chem. Commun.* **1968**, 1585. (b) Torring, E. Z. *Naturforsch. Teil A* **1968**, *23*, 777. (c) Anderson, J. S.; Ogden, J. S. *J. Chem. Phys.* **1969**, *51*, 4189. (d) Hastie, J. W.; Hauge, R. H.; Margrave, J. L. *Inorg. Chim. Acta* **1969**, *3*, 601. (e) Manson, E. L., Jr.; Clark, W. W.; DeLucia, F. C.; Gordy, W. *Phys. Rev.* **1977**, *A15*, 223. (f) Lovas, F. J.; Kaki, A. G.; Olson, W. B. *J. Mol. Spectrosc.* **1981**, *87*, 449.

(8) Botschiwina, P.; Rosmus, P. *J. Chem. Phys.* **1985**, *82*, 1420.

(9) (a) Honing, R. E. *J. Chem. Phys.* **1934**, *22*, 1610. (b) Tsong, T. T. *Appl. Phys. Lett.* **1984**, *45*, 1149. (c) Tsong, T. T. *Phys. Rev.* **1984**, *B30*, 4946. Martin, T. P.; Schaber, H. *J. Chem. Phys.* **1985**, *83*, 855. (d) Bloomfield, L. A.; Freeman, R. R.; Brown, W. L. *Phys. Rev. Lett.* **1985**, *54*, 2246.

(10) (a) McLean, A. D.; Liu, B.; Chandler, G. S. *J. Chem. Phys.* **1984**, *80*, 5130. (b) Raghavachari, K. *J. Chem. Phys.* **1985**, *83*, 3525. (c) Grev, R. S.; Schaefer, H. F., III *Chem. Phys. Lett.* **1985**, *119*, 111. (d) Diercksen, G. H. F.; Gruner, N. E.; Oddershede, J.; Sabin, J. R. *Chem. Phys. Lett.* **1985**, *117*, 29. (e) Raghavachari, K. *J. Chem. Phys.* **1986**, *84*, 5672. (f) Balasubramanian, K. *Chem. Phys. Lett.* **1986**, *125*, 400. (g) Pacchioni, G.; Koutecky, J. *J. Chem. Phys.* **1986**, *84*, 3301. (h) Balasubramanian, K. *Chem. Phys. Lett.* **1987**, *135*, 283.

(11) (a) Lembke, R. R.; Ferrante, R. F.; Weltner, W. *J. Am. Chem. Soc.* **1977**, *99*, 416. (b) Van Zee, R. J.; Ferrante, R. F.; Weltner, W. *Chem. Phys. Lett.* **1987**, *139*, 426.

(12) DeKock, R. L.; Yates, B. F.; Schaefer, H. F., III *Inorg. Chem.* **1989**, *28*, 1680.

(13) Schlegel, H. B. *J. Comput. Chem.* **1982**, *3*, 214.

(14) Hariharan, P. C.; Pople, J. A. *Theor. Chim. Acta* **1973**, *28*, 213.

(15) Frisch, M. J.; Pople, J. A.; Binkley, J. S. *J. Chem. Phys.* **1984**, *80*, 3265.

(16) Krishnan, R.; Binkley, J. S.; Seeger, R.; Pople, J. A. *J. Chem. Phys.* **1980**, *72*, 650. Clark, T.; Chandrasekhar, J.; Spitznagel, G. W.; Schleyer, P. v. R. *J. Comput. Chem.* **1983**, *4*, 294. Frish, M. J.; Pople, J. A.; Binkley, J. S.; *J. Chem. Phys.* **1984**, *80*, 3265.

(17) McLean, A. D.; Chandler, G. S. *J. Chem. Phys.* **1980**, *72*, 5639.

(18) Krishnan, R.; Pople, J. A. *Int. J. Quantum. Chem.* **1978**, *14*, 91.

(19) Pople, J. A.; Head-Gordon, M.; Raghavachari, K. *J. Chem. Phys.* **1987**, *87*, 5958.

(20) Frisch, M. J.; Head-Gordon, M.; Trucks, G. W.; Foresman, J. B.; Schlegel, H. B.; Raghavachari, K.; Robb, M. A.; Binkley, J. S.; Gonzalez, C.; DeFrees, D. J.; Fox, D. J.; Whiteside, R. A.; Seeger, R.; Melius, C. F.; Baker, J.; Martin, R. L.; Kahn, L. R.; Stewart, J. J. P.; Topiol, S.; Pople, J. A. *Gaussian 90*; Gaussian Inc.: Pittsburgh, 1990.

(21) Bruna, P. J.; Peyerimhoff, S. D.; Buenker, R. J. *J. Chem. Phys.* **1980**, *72*, 5437.

(22) (a) Yamada, C.; Saito, S.; Kanamori, H.; Hirota, E. *Astrophys. J.* **1985**, *290*, L65. (b) Yamada, C.; Kanamori, H.; Horiguchi, H.; Tsuchiya, S.; Hirota, E. *J. Chem. Phys.* **1986**, *84*, 2573. (c) Ohishi, M.; Suzuki, H.; Ishikawa, S.-I.; Yamada, C.; Kanamori, H.; Irvine, W. N.; Brown, R. D.; Godfrey, P. D.; Kaifu, N. *Astrophys. J.* **1991**, *380*, L39.

(23) Brown, R. D.; Rice, E. H. N. *J. Am. Chem. Soc.* **1984**, *106*, 6475.

(24) (a) Brown, R. D.; Godfrey, P. D.; Elmes, P. S.; Rodler, M.; Tack, L. M. *J. Am. Chem. Soc.* **1985**, *107*, 4112. (b) Tang, T. B.; Inokuchi, H.; Saito, S.; Yamada, C.; Hirota, H. *Chem. Phys. Lett.* **1985**, *116*, 83. (c) Brown, R. D.; Godfrey, P. D.; Cragg, D. M.; Rice, E. H. N.; Irvine, W. M.; Friberg, P.; Suzuki, H.; Ohishi, M.; Kaifu, N.; Morimoto, M. *Astrophys. J.* **1985**, *297*, 302. (d) Brown, R. D.; Pullin, D. E.; Rice, E. H. N.; Rodler, M. J. *J. Am. Chem. Soc.* **1985**, *107*, 7877. (e) McNaughton, D.; McGilvery, D.; Shanks, F. *J. Mol. Spectrosc.* **1991**, *149*, 458.

(25) Presilla-Marquez, J. D.; Graham, W. R. M. *J. Chem. Phys.* **1992**, *96*, 6509.

(26) Rittby, C. M. L. *J. Chem. Phys.* **1992**, *96*, 6788.

(27) Yu, M. L.; Eldridge, B. N. *Phys. Rev. Lett.* **1987**, *58*, 1691.

(28) Kirby, R. E.; Lichtman, L. *Surf. Sci.* **1974**, *41*, 447.

(29) (a) Schell-Sorokin, A. J.; Demuth, J. E. *Surf. Sci.* **1985**, *157*, 273. (b) Nishijima, M.; Edamoto, K.; Kubota, Y.; Kobayashi, H.; Onchi, M. *Surf. Sci.* **1985**, *158*, 422.

(30) Yasaitis, J. A.; Kaplow, R. *J. Appl. Phys.* **1972**, *43*, 995.

(31) Bianconi, A.; Bauer, R. S. *Surf. Sci.* **1980**, *99*, 76.